THE STATIC ANALYSIS OF COMPOSITE AIRCRAFT WING-BOX STRUCTURE

Asst. Prof. Dr. Ahmed A. Ali
Mechanical Eng. Dept. , College of Eng.
Baghdad University, Bagdad, Iraq

Asst. Lect. Azhar K. Farhood
Mechanical Eng. Dept. , College of Eng.
Baghdad University, Bagdad, Iraq

ABSTRACT

In this paper, the static analysis for finding the best location of boxes inside the composite wing-box structure has been performed. A software ANSYS (ver.11) was used to analyses the Aluminum wing to find the maximum stresses reached in.

These results are used as a base for the composite wingbox to find the numbers of layers and location of the box beam and its dimensions so that the composite wingbox may carry the same loading conditions in the Aluminum wing. Analysis showed that a composite wingbox having two boxes is better than the single or triple boxes wing based on stress to weight ratio. Mass saving of (40%) had been achieved when composite wing-box is used instead of Aluminum wing.

الخلاصة

يتضمن البحث ايجا د افضل موقع للصندوق داخل الجناح الصندوقي المركب من خلال التحليل السكوني للهيكل. أستخدم برنامج (ANSYS11) لايجاد اعلى اجهاد يتحمله جناح الالمنيوم.

هذه النتائج استخدمت كأ ساس في تصميم الجناح الصندوقي المركب لايجاد عدد الطبقات وموقع وابعاد الصندوق وبذلك سوف يتعرض النموذج لنفس الحمل المسلط على الجناح القياسي. بينت التحاليل بأن الجناح المركب الحاوي على صندوقين افضل من الأحادي و الثلاثي و ذلك اعتمادا على النسبة بين الإجهاد / الوزن وان النقصان الواضح في قيمه الكتله عند استخدام الجناح الصندوقي المركب بدل من جناح الالمنيوم القياسي كان بمقدار(٤٠%).

Keywords: wing-box, aircraft structure, composite wing

1. Introduction

As today's military aircraft are required to fly faster, higher and a further, the trend in the wing boxes of such aircraft is towards lighter and thinner structures. One factor which is helping to achieve these aims is the emerging use of composite materials in the primary structure of aircraft because they have a greater strength/weight ratio than conventional aluminum alloys. The use of a multi box wing for the wing box helps meet the requirement for thinness by allowing low wing box depths while still achieving the necessary bending rigidity.

Snell and Bartholomew 1987 studied the minimum weight design of multidirectional carbon fiber reinforced plastic (CFRP) plates under uniaxial compression was first considered. The results of this study were applied to the optimization of multi-spar wing bend boxes under bending and vertical shear loading, using geometric programming. Based on the present simplified modeling, overall weight savings proportional to the material densities of the order of 40% can therefore be expected from the use of composite materials in corrugated spars.

Greenhalgh et-al 1993 Concluded that beneficial twist-bend coupling can be induced in wing box-beam members using conventional continuous fiber fabrication processes. Experimental tests were conducted on five beams to determine beam twist and bend as a function of load at various fiber angle layups. The maximum twist-bend coupling was exhibited at a layup angle of approximately 17°.

Astonused and Williams 1994 presented the buckling analysis of multi-spar wing boxes made from composite materials. Used the lower bound method and the repetitive analysis method. Both methods were illustrated by using the computer program VICONOPT to analyze six variants of a laboratory test specimen of the type used when developing multi-spar wing boxes. The results indicate that the lower bound method usually achieves accuracy well within 10%.

Peter et-al. 2000 established the aeroelastic effects of variation of composite fiber orientation, root flexibility, and stacking of plies for a rectangular closed thin-walled wing box. Used the finite element code ASTROS. The research showed that the root stiffness had a significant influence on the modal response of a wing. It also showed that this behavior influenced the aeroelastic properties of the lifting surface.

Guo et-al. 2003 presented an analytical study on optimization of a laminated composite wing structure for achieving a maximum flutter speed and a minimum weight without strength penalty. Results from a thin-walled wing box made of laminated composite material show that up to 18 per cent increase in flutter speed and 13 per cent reduction in weight can be achieved without compromising the strength. The investigation shows that a careful choice of initial lay-up and design variables leads to a desirable bending, torsional and coupling rigidities, with the provision of an efficient approach when achieving a maximum flutter speed with a minimum mass of a composite wing.

Koundouros et-al. 2004 used the finite element method in conjunction with the Soutis-Fleck model to predict the residual strength after impact of a carbon-fiber reinforced plastic wingbox subjected to a cantilever type loading. The maximum stress failure criterion further validates the Soutis-Fleck model predictions. The Soutis-Fleck model predicts that the wingbox fails at approximately 5.5% less than the experimental observation.

Rohani 2004 presented an investigation on the design and optimization of a thin composite wing box structure for a civil tilt-rotor aircraft. Two different concepts are considered for the cantilever wing: (a) a thin monolithic skin design and (b) a thick sandwich skin design. The global-local technique was used in the analysis and optimization of the six design models. The optimum skin ply pattern for the monolithic skin concept is found to be ((0/±45/90/ (0/90)2) s) s while for the sandwich skin concept the optimal ply pattern was found to be ((0/±45/90)2s)s.

Buchanan 2007 investigated the use of a structural design optimization process to develop an alternative light weight design for a wing box rib. The approach utilized accepted finite element analysis procedures in two iterative loops to derive structures by formulation of a design optimization problem. Definition of a CAD model of the final concept provided indication that a weight saving of approximately 10% over traditional design approaches could be obtained.

Ryu et-al. 2008 noticed the deformation of the composite wing box under bending load was monitored in real time by using the built-in fiber Bragg grating strain sensors. The measured strains showed good agreement with those by twenty electrical strain gages. Also, the experimental results were analyzed and compared with the results simulated by a finite element method. Bending-induced buckling occurred in the wing box and the embedded fiber Bragg gration sensors successfully monitored the buckling behaviors of the top skin and front spar.

The objective of this paper built up the best boxes inside the wing box structure by using software (ANSYS11), based on changing the number of layers, orientation and number of boxes, manufacturing a composite wing box from (E-glass) that may carry the same loading condition for the standard Aluminum wing and having a less weight than the Aluminum wing.

2. Wing Specification

In this work an Aluminum model is constructed to obtain the maximum load that may be carried by the standard wing that makes the stress reaches its maximum or ultimate value in the root of the wing. This value of load is used in the composite wingbox model design to estimate the best location (as shown in **Fig.1)** of the boxes inside wing section. **Table 1** and **Fig.2** shows the wing body configuration data [11].

3. Beam Used in The Wing Standard Structure.

Properties of the beam section used in building the wing longitudinal stiffeners are shown in **Table 2.**

4. Materials Used in the Wing Structure.

The properties of the isotropic materials used in building the wing structure are shown in **Table 3.**

5. Finite Element Analysis of Standard Aircraft Wing

The finite element analysis will be used to obtain the displacement, stress, as they are considered the main design parameters. The wing will be divided into elements for the isotropic shell structure the element (4-node quadrilateral element) had been used. The elements shell 63 and beam 4 are used for wing standard as Shown in **Table 4** .

6. Structural Model

The structural model used in this work is in the form of a two boxes, fiber-reinforced composite wingbox shown in **Fig.3**.The considered structure model is similar to that developed in Ref.[12].**Table 5** shows experimental mechanical properties of woven glass fibers.

7. Element Type of the Model

The composite wingbox of the aircraft consists of box, ribs, as well as lower and upper skin, so the wing will be divided into elements for the orthotropic shell structure, where the element (8-node octeral element) as shown in **Fig.4** had been used for modeling.

Each node on this element has six degree of freedom (three translation and three rotation). The region of the wing root are built in so (u = v = w $=\theta_x = \theta_y = \theta_z = 0$). For the analysis of the three dimensional model, the finite element tool (ANSYS 11) is used. The element shell 99 is used for wing model. A convergence in the numerical results calculated by ANSYS is achieved after using (29374)D.O.F , where the value of stress shows a good stability in this range as shown in **Fig.5**.

8. Experimental work

The primary objective of the methodology is to obtain the deflection of the composite wing box model structure, subjected to transverse static load and calculating the deflection at the tip end of the wing using an LCD CAMERA (12 mega pixel) having a resolution of 0.001474 mm/pixel for each image captured by the camera, the rig for the experimental work as illustrated in **Fig.6** .The load is applied as a concentrated force on the tip end from 1to 11 kg by steps of 1kg each as shown in **Fig.7**, images are captured for each step of loading and where analyzed to calculate the difference in pixels between each step of loading. This difference is multiplied by the resolution to obtain the deflection for each step of loading. The results are compared with the tradition way of monitoring deflection using DIAL GAGE having a accuracy of 0.01mm as shown in **Fig.8**. The results shows a good agreement, these results are compared with the numerical results obtained by ANSYS11 and little difference between them was observed this difference is due to the miss contact between some parts in the experimental model which plays a big part in reducing the stiffness of the model.

9. Results

Structure analysis Package ANSYS was used to examine the best box (one box, two boxes and three boxes) and better location of the boxes inside the wing from the less stress to weight Ratio, as well as the less stress of fiber orientation and number of layer for composite material under static load. Experimental program was used to estimate the deflection and to compare it with the numerical results.

10. The Best Location of Boxes inside the Wing

A structure analysis was achieved by using ANSYS11 in order to study wingbox in static loading condition. The analysis results for one box of composite material and its results are shown in **Table 6** and **Fig. 9**, In case 40% for cord length(C) can be noticed that this ratio gives the best location of one box because the stress to weight ratio is (7.628129) which is less than the other ratios.

Also **Tables 7** and **8** show the best location of two and three boxes, where the case 31%cord is the better for two boxes while the results for three boxes is at 35%cord.

Figs. 9, 10 and **11** shows the smaller ratio of the one box, two boxes and three boxes inside the wing, where in **Table 9** the ratio for the two boxes is the best because the minimum value is (6.873) at 31%cord, as well as the deflection which are less than the one boxes at 40%cord and three boxes at 35%cord.

11. The Effect of Fiber Orientation for The Two Boxes Wing

An optimization analysis based on varying the orientation of the four layers of woven fiber for the two box section is done in this work. That the fiber orientation (90/0/0/90) has a minimum value of stresses which is (74.5Mpa) at the root for composite wingbox as shown in **Fig.12** when compared with other fiber orientation, therefore it is a good orientation.

12. Structural Testing

A tailored composite wing box for methodology was subjected to transverse static load at the tip. **Tables 10** and **11** show the experimental and numerical results for six layers (two layers for skin and four layers for the box), of the two boxes with over all thickness (4mm). When changing the load for each case there is a little deference between the value of the displacements measured numerically and experimentally, this is due to the miss in contact between the various parts of the wing as shown in **Figs. 13** and **14**.

Fig. 15 shows the deflection shape for the wing box model obtain from numerical analysis by ANSYS at maximum loading.

13. Conclusions

The main conclusions obtained from the present work can be summarized as follow:

1. From the results obtained from ANSYS software it's found that the wingbox with double boxes section is better than the single and triple boxes section from the side that the double boxes section has a stress to weight ratio (9.9% and 1.0196%) less than the other sections respectively.
2. The composite double box wing section has a (40%) less weight than the traditional Aluminum wing which carries the same loading condition.
3. The orientation of the woven fibers (90, 0, 0, 90) for the inside boxes gives the minimum stress compared with the other orientations.
4. In the case of the single box section the dimensions of the box should be 40% of cord length to give the minimum stress /weight ratio, whereas for double box section the ratio is 31% of the cord length and for the triple section the ratio is 35%.
5. In calculating the minimum number of layers needed in constructing the interior boxes that will carry the same load, the Aluminum wing results show that choosing two or three layers makes the stress reach the region of ultimate stress. Therefore, four layers had been chosen to make the stress within the range of allowable value.
6. The use of digital LCD camera in measuring deflection is more accurate from the dial gage where an accuracy of 0.001474 mm/pixel had been achieved.
7. The use of tapered composite wingbox section is easier in constructing and manufacturing from a rectangular composite wingbox section.

14. References

Chi-Young Ryu, Jung-Ryul Lee, Chun-Gon Kim and Chang-Sun Hong "Buckling behavior monitoring of a composite wing box using multiplexed and multi-channeled built-in fiber bragg grating strain sensors", NOT&International 41, (2008), 534-543.

E. S. Greenhalgh, C. M. Pastore and M. Garfinkle "A continuous-fiber composite wing box-beam exhibiting twist-bend coupling", composite engineering, vol.3, Nos 7-8, pp.691-697, 1993.

G. Aston and F. W. Williams "Simplified methods for the buckling analysis of composite multi-spar wing boxes", Composite Structures28, (1994), 215-223.

Guo S.J., Bannerjee J.R. and Cheung C.W. "The effect of laminate lay-up on the flutter speed of composite wings", Journal of aerospace engineering, vol.217, No.(3), pp115-122, 2003.

Lie Qiu and Shenfang Yuan "On development of a multi-channel PZT array scanning system and its evaluating application on UAV wing box", Sensors and Actuators A 151 (2009) 220–230.

M. B. Snell and P. Bartholomew "The engineering optimization of hybrid composite/metallic wing boxes for buckling and strength constraints", Composite Structures7, (1987), 21-58.

MasoudRais-Rohani "Global-local analysis and optimization of a composite civil tilt-rotor wing", NASA Langley grant NAG 1-1571,2004.

Megson T.H.G "Aircraft structure for engineering students" Arnold, 1999.

Michael Koundouros, Brian G. Falzon, Costas Soutis and Steven J.Lord "Predicting the ultimate load of a CFRP wing box", composite: part A35, (2004), 895-903.

Peter W. G. De Baets, Rupinder S. Battoo and Dimitri N. Mavris "Aeroelastic analysis of a Composite wing box with varying root flexibity", AIAA-2000-1623.

Shijun Guo "Aeroelastic optimization of an aerobatic aircraft wing structure", Aerospace Science and Technology 11 (2007) 396–404.

Sid Buchanan "Development of a wing box rib for a passenger Jet aircraft using design optimization and constrained to traditional design and manufacture requirements", Altair Engineering, 2007.

Table (1) Wing body configuration data.

Wing span(m)	4.6
Aspect ratio	6.7
Taper ratio	0.44
Root chord(m)	2.03
Tip chord(m)	0.8932
Wing root section profile	NACA 23015
Wing tip section profile	NACA 23012
Wing shape	Trapezoidal

Table (2) Properties of beam section [11].

Beam section type	Representation	Cross sectional area(m^2)	$I_{xx}(m^4)$	$I_{yy}(m^4)$
	stringers	$69*10^{-6}$	٠.75418*10^{-8}	٠.13387*10^{-8}

Table (3) Properties of the isotropic material [11].

Material	Young modulus(Gpa)	Yield stress(Mpa)	Poisson Ratio	Density(kg/m3)
[AL]7075-T6	71	470	0.33	2800

Table (4) Finite element of the wing

Parts	Type of element(ANSYS11)
Surface(isotropic)	Shell63(4-node quadrilateral element)elastic shell
Ribs	Shell63(4-node quadrilateral element)elastic shell
Spars	Shell63(4-nodequadrilateral element)elastic shell
Stringers	Beam 4(3-D elastic beam)

Table (5) Experimental mechanical properties.

composite	E_x (Gpa)	E_y (Gpa)	σ_{yeild} (Mpa)	υ_{xy}	υ_{yz}	G_{xy} (Gpa)
Woven fiber	38	38	227.1	0.23	0.053	5.3

Table (6) Results of optimization for one box section.

One box					
cases	**%c**	**Deflection (m)**	**Stress (Mpa)**	**Weight (kg)**	**Ratio (σ/w)**
1	9	0.395724	143	17.20267	8.312663
2	18	0.394092	146	17.6276	8.282466
3	22	0.395176	145	17.4785	8.295906
4	31	0.401061	131	17.1381	7.643788
5	40	0.413952	128	16.76	7.628129
6	49	0.429199	176	16.45	11.6991
7	58	0.457167	231	16.1414	14.311
8	76	0.517133	159	15.38111	10.3373355

Table (7) Results of optimization for two boxes sections.

Two box					
cases	**%c**	**Deflection (m)**	**Stress (Mpa)**	**Weight (kg)**	**Ratio (σ/w)**
1	18	0.372529	128	18.53	6.91
2	31	0.37535	124	18.0416	6.873
3	36	0.37765	130	17.872	7.274
4	45	0.387795	134	17.5422	7.639
5	49	0.3912926	135	17.353	7.78

Table (8) Results of optimization for three boxes sections.

		Three box			
cases	%c	Deflection (m)	Stress (Mpa)	Weight (kg)	Ratio (σ/w)
1	27	0.381653	129	18.21203	7.08323
2	35	0.382764	126	18.14568	6.9438
3	67	0.38509	137	17.1743	7.977035

Table (9) A comparison between the three types of wings showing the stress to weight ratios and box dimensions relative to cord

Types	Stress(Mpa)	Weight(kg)	Ratio (Mpa/kg)	Dimension relative to cord length %
One box	128	16.76	7.62813	40%
Two boxes	124	18.0416	6.873	31%
Three boxes	126	18.14568	6.9438	35%

•

Table (10) Experimental determination of the deflection at the tip of the composite wingbox experimentally using (camera) and Ansys, (2skin layers and 4layers for box),4mm thickness.

		Deflection(mm)		
case	Load(kg)	Experimental(Camera)	ANSYS(ver.11)	Error%
1	1	0.1322	0.118	10.74%
2	2	0.26532	0.236	11.05%
3	3	0.39	0.354	9.23%
4	4	0.50434	0.472	6.4%
5	5	0.66	0.59	10.6%
6	6	0.8	0.708	11.5%
7	7	0.9125	0.826	9.48%
8	8	1.06	0.964	10.9%
9	9	1.15	1.062	7.65%
10	10	1.3	1.18	9.23%
11	11	1.4	1.298	7.28%

Table (11) Experimental determination of the deflection at the tip of the composite wingbox experimentally using (camera) and dial gage ,(2skin layers and 4layers for box),4mm thickness.

		Deflection(mm)		
case	Load(kg)	Dial gage	Camera	Error%
1	1	0.145	0.1322	8.8276%
2	2	0.292	0.26532	9.137%
3	3	0.4	0.39	2.5%
4	4	0.55	0.50434	8.3%
5	5	0.695	0.66	5.036%
6	6	0.86	0.8	6.977%
7	7	0.95	0.9125	3.95%
8	8	1.18	1.06	10.17%
9	9	1.25	1.15	8%
10	10	1.4	1.3	7.143%
11	11	1.52	1.4	7.9%

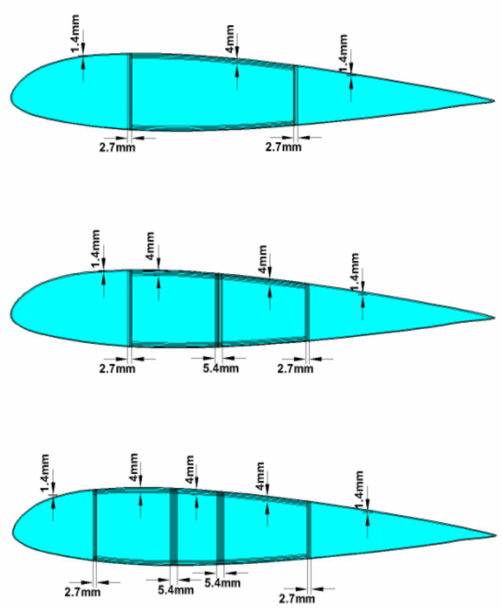

Figure (1) Types of the wing box sections.

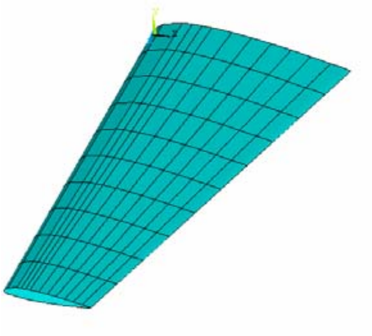

Figure (2) Shape of standard wing.

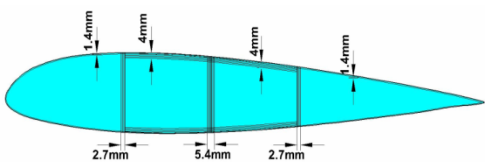

Figure (3) Composite wingbox.

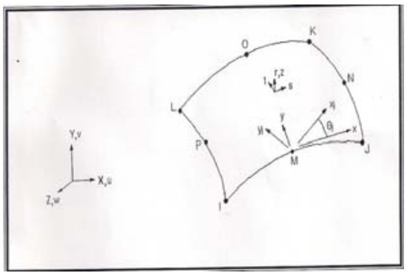

Figure (4) Element - 8nodes.

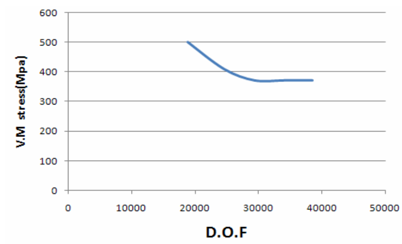

Figure (5) Stability of results for taper wingbox.

Figure (6) Using digital camera for calculating deflection.

Figure (7) Rig used for the experimental work

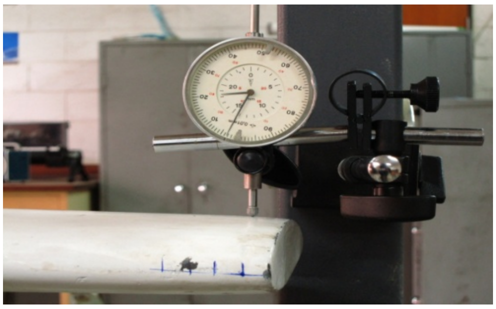

Figure (8) Dial Gage for measuring tip deflection.

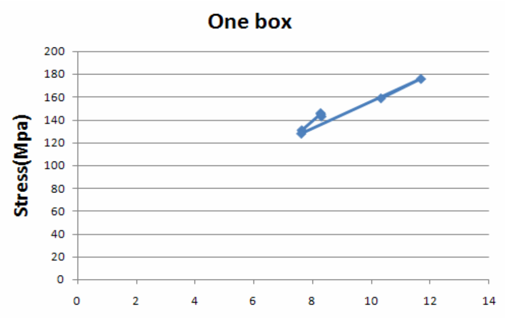

Figure (9) Stress to weight ratio for one box section.

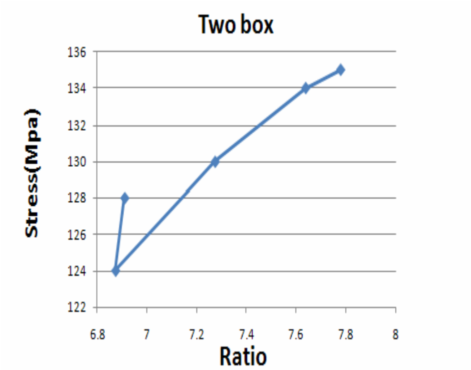

Figure (10) Stress to weight ratio for two boxes section.

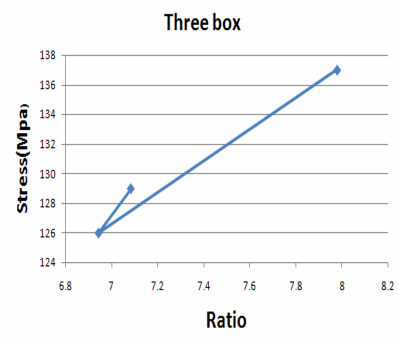

Figure (11) Stress to weight ratio for three boxes section.

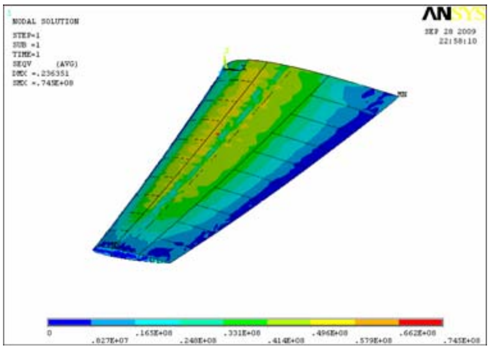

Figure (12) Minimum value of stress at the wing root with (90/0/0/90) fibers orientation.

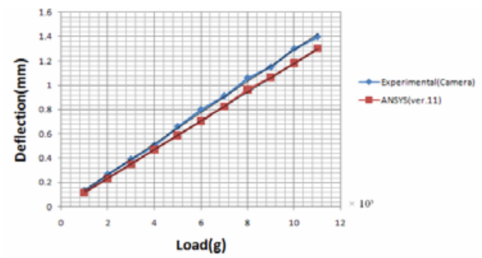

Figure (13) Measured deflection by the camera and ANSYS.

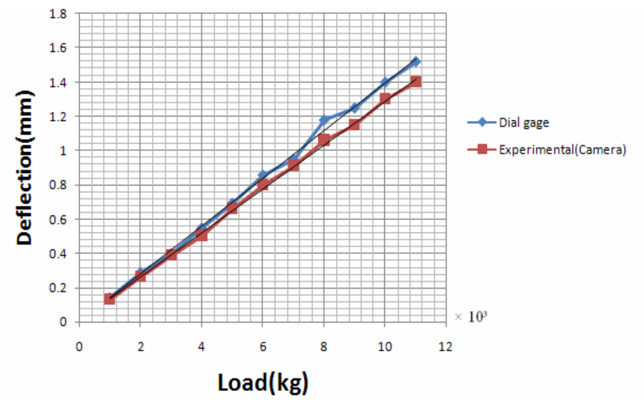

Figure (14) Measured deflection by the camera and Dial gage.

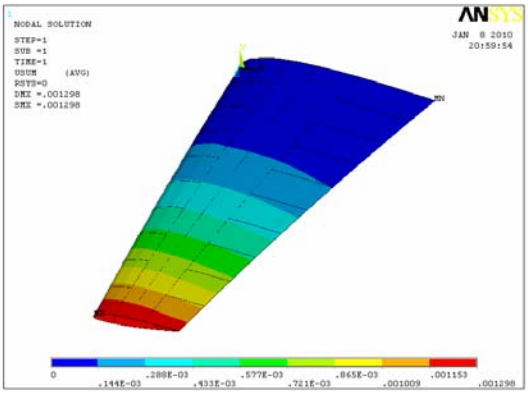

Figure (15) Deflected shape of model at maximum load for.